In-silico media optimization for continuous cultures using genome scale metabolic networks: the case of CHO-K1

Bárbara Ariane Pérez-Fernández[1], **Jorge Fernández-de-Cossio-Díaz**[1,2], **Tammy Boggiano**[2],**Kalet León**[2], **Roberto Mulet**[1]

1 Group of Complex Systems and Statistical Physics. Department of Theoretical Physics, Physics Faculty, University of Havana,Cuba

2 Systems Biology Department, Center of Molecular Immunlogy, Havana, Cuba

Abstract

The cell culture is the central piece of a biotechnological industrial process. It includes upstream (*e.g.* media preparation, fixed costs, etc.) and downstream steps (*e.g.* product purification, waste disposal, etc.). In the continuous mode of cell culture, a constant flow of fresh media replaces culture fluid until the system reaches a steady state. This steady state is the standard operation mode which, under very general conditions, is a function of the ratio between the cell density and the dilution rate and depends on the media supplied to the culture. To optimize the production process it is widely accepted that the concentration of the metabolites in this media should be careful tuned. A poor media may not provide enough nutrients to the culture, while a media too rich in nutrients may be a waste of resources because, either the cells do not use all of the available nutrients, or worse, they over-consume them producing toxic byproducts. In this work we show how an in-silico study of a genome scale metabolic network coupled to the dynamics of a chemostat could guide the strategy to optimize the media to be used in a continuous process. Given a known media we model the concentrations of the cells in a chemostat as a function of the dilution rate. Then, we cast the problem of optimizing the production process within a linear programming framework in which the goal is to minimize the cost of the media keeping fixed the cell concentration for a given dilution rate in the chemostat. We evaluate our results in two metabolic models: first a simplified model of mammalian cell metabolism, and then in a realistic genome-scale metabolic networks of mammalian cells, the Chinese Hamster Ovary (CHO) cell line. We explore the later in more detail given specific meaning to the predictions of the concentrations of several metabolites.

Keywords: metabolic networks, cell culture, chemostat

Introduction

There are three dominant modes of cell culture operation for protein production: batch, fed-batch, and continuous culture. The batch mode of operation is a closed system in which a fixed amount of nutrients is added at the beginning of the culture until the cells starve. In fed-batch cell culture, the nutrients are added at discrete time intervals. In the continuous mode, a constant flow of fresh media replaces continuously the culture fluid keeping the bioreactor volume constant.

While at present, a large part of the biotechnological industry adopts batch or fed-batch processes, the advantages of continuous processing are strongly defended in the literature (Griffiths, 1992; Werner et al., 1992). Indeed, several authors agree that the continuous mode will be used extensively in the near future (Fernandez-de-Cossío-Díaz et al., 2017; K. B. Konstantinov & Cooney, 2015; Werner et al., 1992).

Optimal performance of a perfusion filtration system requires efficient retention of cells, and keeping this can be expensive and hard to model. However, there is a classic example of continuous cell culture without cell retention, the *chemostat*, where the media is added at a constant flow rate and the bioreactor content is removed at the same flow rate (Henry et al., 2008). A recent study (Fernandez-de-Cossío-Díaz et al., 2017) showed that the steady-state cellular metabolism is equivalent in the chemostat and in any perfusion system with a non-zero bleeding rate (ϕ), indicating that the chemostat is an ideal experimental model of high density perfusion cell culture.

Commonly, in continuous cell cultures the same media composition is provided for different dilution rates. However, depending on the cell density X and the dilution rate D at which the culture is found, the cells will adopt different metabolic phenotypes and therefore may need different nutrients and in different concentrations. Moreover, the amino acids supplied to the cell culture do not have the same price. Some of them, such as glycine, are cheaper, while others, like glutamine, are more expensive. It is not surprising that media design is an attractive alternative to significantly modulate metabolic transitions and decrease the costs of the production process. Indeed, the development of the biotechnology industry has boosted and encouraged efforts to improve cell culture media to maximize product yields and reduce the cost of goods (Jerums & Yang, 2005).

Currently the optimization of culture media is mainly based on empirical methods. *Component titration* is a standard approach to improve a medium. This method involves a series of experiments to determine the "dose response"of a cell line to various components of the medium by adding

each one in varying amounts to individual cultures. *Media combination* is another method, which quickly generates many new media simply by combining existing formulations, such that process developers can quickly focus on the best combination. Another widely used method is the *analysis of spent media*, which can provide important information through chemical analysis to measure how a medium changes during the culture process. By analyzing spent media, process developers can make calculations that describe both nutrient depletion and metabolite accumulation (Jerums & Yang, 2005). However, despite the large number of results and findings, more specific work is required, specially for mammalian cell cultures (Brühlmann et al., 2015). In this work we hope to contribute to this task showing that, starting from an in-silico perspective it is possible to guide experimentalists on the selection process for the metabolites and their concentrations and at the same time to decrease the waste of material resources. We argue that it is possible to exploit the information available on *genome scale metabolic networks* to optimize a cell culture.

Various methodologies have been created to predict the cellular metabolism based on the stochiometry of metabolic networks. For example, Flux Balance Analysis (FBA) provides a solution space that contains all the possible steady-state flux distributions that satisfy the applied constraints. Within this space FBA selects, using Linear Programming, the one that maximizes an objective function, typically cell growth or biomass synthesis (Varma & Palsson, 1994).

Although FBA is a powerful tool to predict cell metabolism in the growth phase (Feist & Palsson, 2010; Ibarra et al., 2002,?; Sheikh et al., 2005; Shlomi et al., 2011) it fails to predict the existence of metabolic transitions that have been observed in several experiments (Vazquez & Oltvai, 2016). These transitions are very relevant in cell cultures, because they affect the consumption or secretion of metabolites and the set of nutrients that limit growth (Fernandez-de-Cossío-Díaz et al., 2017). An extension of FBA considers molecular crowding (FBAwMC) assuming that enzymes have a maximum turnover number. This molecular crowding naturally results in a constraint on the total metabolic flux through the network (Hoek & Merks, 2012). In practice, it means that the total flux through the metabolic network is limited (Beg et al., 2007). This extension predicts transitions to less efficient metabolic pathways from the viewpoint of energy units generated per unit of substrates consumed and reflects a more realistic behaviour of cellular metabolism.

In this work, we use FBAwMC to model the internal metabolism of cells in a continuous culture and couple this metabolism with the macroscopic variables that characterize a chemostat. Within

this framework we optimize, *in the sense of producing a media of minimum cost*, the metabolic concentrations that must be supplied to the cell culture at a fixed rate of biomass synthesis. We test our approach for two genome-scale metabolic networks and for a simplified network of mammalian cell metabolism, but the methodology is easily extensible to other cell lines. We obtained qualitative similar results in the three systems studied and our predictions suggest novel strategies to decrease the costs of continuous bio-manufacturing.

Materials and Methods

Dynamical model of continuous cell culture

We study an homogeneous culture of cells growing inside a well-mixed bioreactor, where fresh media continuously replaces culture fluid (Fig 1). The fundamental dynamical equations describing this system are:

$$\frac{dX}{dt} = (\mu - \phi D)X \tag{1}$$

$$\frac{ds_i}{dt} = -u_i X - (s_i - c_i)D \tag{2}$$

where X denotes the density of cells in the bioreactor (units: gDW/L), μ the effective cell growth rate (units: 1/h), and the bleeding coefficient, ϕ (unit-less), which in perfusion systems characterizes the fraction of cells that escape from the culture through a cell-retention device. The term u_i denotes the specific uptake of metabolite i (units: mmol/gDW/h), and s_i the concentration of metabolite i in the culture (units: mM). The external parameters controlling the culture are the media concentration of metabolite i, c_i (units: mM) and the dilution rate, D (units: 1/h).

Equation (1) describes the dynamics of cell density as a balance between cell growth and dilution, while equation (2) describes the dynamics of metabolite concentrations in the culture as a balance between cell consumption (or excretion if $u_i < 0$) and dilution (Fernandez-de-Cossío-Díaz et al., 2017).

Under quite general conditions, it can be shown that for a system of the form (Eq. 1-2), the steady state is a function of the ratio $\xi = X/D$, which is therefore and ideal control parameter of

the system. In particular, this implies that the steady states of a perfusion system (with $0 < \phi < 1$) map to those of a chemostat through a simple rule (Fernandez-de-Cossío-Díaz et al., 2017). Since our results are qualitatively invariant to changes in ϕ, we set $\phi = 1$ in what follows.

If S_{ik} denotes the stoichiometric coefficient of metabolite i in reaction k ($S_{ik} > 0$ if metabolite i is produced in the reaction, $S_{ik} < 0$ if it is consumed), and r_k is the flux of reaction k, then the metabolic network produces a net output flux of metabolite i at a rate $\sum_k S_{ik} r_k$, where $S_{ik} = 0$ if metabolite i does not participate in reaction k. This output flux must balance the cellular demands for metabolite i. In particular we consider a constant maintenance demand at rate e_i which is independent of growth, as well as the requirements of each metabolite for the synthesis of biomass components. If y_i units of metabolite i are needed per unit of biomass produced, and biomass is synthesized at a rate Z, we obtain the following overall balance equation for each metabolite i (Fernandez-de-Cossío-Díaz et al., 2017):

$$\sum_k S_{ik} r_k + u_i = e_i + y_i Z \quad \forall i \tag{3}$$

In Eq.(3), we are assuming that metabolites inside the cell attain quasi-steady state concentrations (Edwards et al., 2002), so that fluxes of intra-cellular metabolic reactions balance at each metabolite.

As in FBAwMC, we consider that cells have a limited enzyme budget (Noor et al., 2016). The synthesis of new enzymes, needed to catalyze many intracellular reactions, consumes limited resources, including amino acids, energy, cytosolic or membrane space (for enzymes located on membranes), ribosomes, all of which can be modeled as generic enzyme costs (Molenaar et al., 2009; Vazquez & Oltvai, 2011). We split reversible reaction fluxes into negative and positive parts, $r_k = r_k^+ - r_k^-$, with $r_k^\pm \geq 0$, and quantify the total cost of a flux distribution in the simplest (approximate) linear form (Fernandez-de-Cossío-Díaz et al., 2017):

$$\alpha = \sum_k \alpha_k^+ r_k^+ + \alpha_k^- r_k^- \leq C \tag{4}$$

where α_k^+ and α_k^- are constant flux costs. The limited budget of the cell to support enzymatic reactions is modeled as a constraint $\alpha \leq C$, where C is a constant maximum cost, according to T. Shlomi et al. (Shlomi et al., 2011). Thermodynamics places additional reversibility constrains on

the flux directions of some intra-cellular reactions, which can be written as:

$$lb_k \leqslant r_k \leqslant ub_k \tag{5}$$

In addition, the specific uptake of each metabolite u_i is also bounded. To take this into account we follow the analysis of Fernandez-de-Cossio-Diaz et al. (Fernandez-de-Cossío-Díaz et al., 2017). For low cell density, nutrients will be in excess and uptakes are only bounded by the maximum uptake rates of each metabolite determined by molecular details of the transport process (V_i). For high cell density, the concentrations of limiting substrates reach very low levels, a new regime appears where cells compete for resources. As the concentrations of the substrates in the culture are always positive ($s_i \geq 0$), the mass balance equation (Eq.(3) in steady state) implies that $u_i \leq c_i/\xi$. Besides, for metabolites that cannot be secreted, the lower bound of u_i is $L_i = 0$, and $L_i = \infty$ otherwise. Then,

$$-L_i \leq u_i \leq \text{Min}(V_i, c_i/\xi) \tag{6}$$

Moreover, the waste secreted by product of fermentation on mammalian cells affect the growth rate μ, and this effect is present in our model. The two toxic byproducts most commonly studied in mammalian cell cultures are ammonia and lactate. Parameters describing these effects quantitatively vary over an order of magnitude depending on culture conditions and cell-line. In our model we incorporate these effects through the factor K and the death rate σ (Fernandez-de-Cossío-Díaz et al., 2017),

$$\mu = Z \times K(s_i) - \sigma(s_i) \tag{7}$$

where, s_i indicate the concentrations of toxic metabolites for culture, and $0 \leq 1 - K(s_i) \leq 1$ represents a fraction of biomass that must be expended on non-growth related activities, for example, due to increased maintenance demands on account of environmental toxicity. Knowing the value of biomass production Z, we obtain the effective cell growth rate μ depending on the concentrations of toxic metabolites in the culture, such as lactate and ammonia (Eq.(7)). In the chemostat, for each stationary state of the Eq.(1), $(\mu - \phi D)X = 0$, $\mu = D$ because $\phi = 1$. In short, the biomass synthesis rate Z is maximized within the constraints given by equations, (3), (4), (5) and (6).

Media Optimization

Above, we described a model(Fernandez-de-Cossío-Díaz et al., 2017) that couples the metabolism of the cells with the external parameters of the chemostat. With this model we can predict, given a reference medium, the concentrations of the culture X as a function of $\xi = X/D$. Here we explain how this can be exploited to optimize the media provided to the cells.

Our goal is to find a medium, of minimum cost, that is able to maintain the steady state of the chemostat predicted using a reference medium, Z. In mathematical terms we want to find the set of c_i such that:

$$C = \text{Min} \quad \sum_i w_i c_i \tag{8}$$

is minimum. Where c_i is the concentration of each nutrient supplied and w_i its cost in the market.

In other words, instead of maximizing Z, as usual in the FBA and FBAwMC frameworks, we minimize the cost of the medium, C, under linear constraints, fixing Z at the value expected by the reference medium. This is done respecting the coupling between the internal metabolism of the cells and the chemostat, as discussed in the previous section.

Economic analysis of the continuous process

According to the literature, the development of economically competitive perfusion processes for the production of stable proteins depends on our ability to reduce the dilution rate while maintaining high cell density. That is, to have processes that operate at low specific perfusion rates ($1/\xi$). This strategy is known as "push-to-low"$1/\xi$ and was introduced by Konstantinov et al.(K. Konstantinov et al., 2006). However, we argue that care must be taken when considering this technique. As the dilution rate decreases, a limit is reached below which the yield decreases due to low cell growth and viability, specific productivity or product instability.

Moreover, in addition to the cost of the media we consider the cost of the production process as a whole, to understand how the steady state of the culture, as a function of ξ, determines the optimal mode of operation of the system. We exploit public data obtained from an economic evaluation realized in the Center of Molecular Immunlogy (CIM) (Torriente, 2014).

To evaluate the production cost in a continuous culture, we consider three components. First,

for a chemostat of volume V working at the dilution rate D the cost of the media supplied at a flow rate VD is $VD\sum_i w_i c_i$. Second, the cost of storage and purification that together with any and other cost growing proportionally with the scale of production (for example: bioreactor maintenance, workers, etc.) is given by: αVD. Finally we consider also a fixed cost per unit time independent of the scale of production, β. In this way, the total cost per unit of time is:

$$\text{cost/time} = (\sum_i w_i c_i)VD + \alpha VD + \beta \tag{9}$$

Moreover, for each VD unit of volume that is supplied to the culture per unit of time, we have VDs_p units of product, where s_p is the concentration of product in the culture. In addition, we know that $Ds_p = q_p X$, where q_p is the cell specific productivity which is defined in units of product obtained per unit of time per cell (Meleady et al., 2011) such that.

$$\text{product/time} = Vq_pX \tag{10}$$

Then, the *cost of the whole process* per unit of product is

$$\Omega = \frac{\text{cost/time}}{\text{product/time}} = \frac{1}{q_p X}\left(D\sum_i w_i c_i + D\alpha + \frac{\beta}{V}\right) \tag{11}$$

Note that Eq.(11) depends on X and D, but since $1/\xi = D/X$ we may write Ω as a function of ξ and X,

$$\Omega(\xi, X) = \frac{1}{q_p}\left(\frac{\sum_i w_i c_i + \alpha}{\xi} + \frac{\beta/V}{X}\right) \tag{12}$$

Metabolic networks

Simplified metabolic network

We analyse first a simplified metabolic network. The goal is to apply our optimization model to a network where it is possible to observe and understand the possible steady states of the metabolism and their implications in the production process of the continuous culture. The simplest network that can be built must use a minimum of two nutrients, because otherwise the optimization of the medium is trivial.

We adapted a simplified metabolic model from (Fernandez-de-Cossío-Díaz & Vazquez, 2017),

which studies the metabolic requirements of growing mammalian cells for two important nutrients, namely glucose and glutamine. The model also considers exchanges of lactate and explains a metabolic transition to fermentation (Warburg effect) as well as the elevated consumption glutamine in spite of it being a non-essential amino acid. Figure 2 presents a detailed diagram of the metabolic processes considered.

The model includes the synthesis of precursors required for biomass production, especifically amino acids, lipids and polysaccharides. It is known that mammalian cells exhibit high rates of glucose fermentation to lactate even when growing in aerobic conditions (Warburg effect). This effect is accompanied by increased glutamine utilization (DeBerardinis et al., 2007) and reductive carboxylation of glutamine to the lipid precursor AcCoA (Mullen et al., 2012). By considering the limits of aerobic metabolism (*i.e.*, the mitocondrial capacity for oxidative phosphorylation), in the context of the energetic requirements of the cell and the NAD/NADH balance, the model explains the glutamine requirements of growing cells as well as the obligatory transition to fermentation (Fernandez-de-Cossío-Díaz & Vazquez, 2017). The simultaneous use of glucose and glutamine as carbon and energy sources, made them an ideal system to study the optimization of a simplified media.

Glucose input is measured in units of ATP produced by glycolysis (one mole glucose = 1/2 mole of ATP). In the aerobic mode, the pathways emerging from glucose and leading to the major biomass precursors (non-essential amino acids, AcCoA, glucose, and nucleotides), result in a net production of NADH from NAD^+, which must be balanced by the oxidation of NADH in the mitochondria (Fernandez-de-Cossío-Díaz & Vazquez, 2017). We consider that the mitochondria oxidise NADH with an ATP yield of approximately 2.5 ATP/NADH.

The oxidation of pyruvate, which takes place in the innermost compartment of the mitochondria (in eukaryote cells), converts pyruvate (three-carbon molecule) into acetyl-CoA (two-carbon molecule bound to coenzyme A) producing a NADH molecule. The addition of CoA helps to activate the acetyl group and prepares it to experience the necessary reactions to enter the citric acid cycle or Krebs cycle. The latter which consists in a series of redox reactions catalysed by enzymes that serve to harness the energy remaining in the acetyl group and is represented in Fig.2 by the letter K.

For the mass balance in ATP synthesis (denoted A in Fig. 2), we consider a maintenance

demand independent of the cell proliferation rate $A_{mant}(\mathrm{mol_{ATP}/gDW/h})$ and take into account the polymerization of precursors A_{pol} ($\mathrm{mol_{ATP}/gDW}$) per unit of biomass that is synthesized at rate Z. The polymerization process is the formation of complicated macromolecules (proteins) from simpler precursors (amino acids). When considering energy demand and polymerization, we get the following expression for the synthesis of ATP,

$$A = A_{pol}Z + A_{mant} \tag{13}$$

Adding up the contributions to transamination (T), dehydrogenation (N), isocitrate dehydrogenase flux (E') and phosphorilation (A), shown in Fig. 2, we arrive at:

$$\begin{aligned}
T &= (c+g+s+a+n+d+r)Z \\
N &= (a+c+g+s+n+d+x)Z + 2E' + 2K + (c+g+s+x)Z + E' \\
&\quad +K + 2K + E' + K - T - E' + (-2p-r)Z \\
N &= (a_1)Z + 6K + -3Q \\
E' &= (q+r+e+p)Z - Q \\
A &= A_1 + A_2 = A_{pol}Z + A_{mant} \\
A_1 &= L + K - Q + (a_2)Z - q'Z \\
A_2 &= 2.5N
\end{aligned}$$

where Z (h^{-1}) represents the biomass synthesis rate; K the flux through the Krebs cycle; G and Q are the uptakes of glucose and glutamine and L the secretion of lactate; $A_{pol}(mol_{\mathrm{ATP}}/gDW)$ is the energy demand corresponding to the polymerization process; and $A_{mant}(mol_{\mathrm{ATP}}/gDW/h)$ is the flux of energy maintenance demand. Lower case letters denote amino-acids in the usual nomenclature, x denotes AcCoa (which we use as the lipid unit), and z denotes glucose. The constants a_1 and a_2 were defined as

$$a_1 = 3(q+e) + p + r + c + g + s + 2x \tag{14}$$

$$a_2 = a + q + e + x - n \tag{15}$$

Next, balancing the inflow and outflow of the *glc* metabolite, we obtain the following equation, for the biomass synthesis rate

$$G + 2Q - L - 2K = a_3 Z \tag{16}$$

where $a_3 = z + a + c + g + s + n + d + x + 2(q + r + p + e)$.

The parameters $A_{pol} = 29\ \mathrm{mmol_{ATP}/gDW}$, $A_{mant} = 0.45\ \mathrm{mmol_{ATP}/gDW/h}$, $a_1 = 15\ \mathrm{mmol_{ATP}/gDW}$, $a_2 = 6.8\ \mathrm{mmol_{ATP}/gDW}$ and $a_3 = 10\ \mathrm{mmol_{ATP}/gDW}$ were obtained by (Fernandez-de-Cossío-Díaz & Vazquez, 2017) from experimental measurements available in the literature.

The dehydrogenation flux N is limited because the production of NADH must be processed in the mitochondria via the electron transport chain. This step is limited by the available intracellular space for the large volume of the enzymes involved. To calculate how much NADH can be oxidized, we took into account the OxPhos capacity of the mitochondria described in (Fernandez-de-Cossío-Díaz & Vazquez, 2017), which leads to the estimate of the dehydrogenation flux limit (conversion of NAD^+ to NADH):

$$N \leq N_{max} = 0.32\ \mathrm{mmol_{NADH}}/gDW/h. \tag{17}$$

In this model, the toxic by-product for cells is lactate, which induces a death rate proportional to its concentration in the culture:

$$\mu = Z - s_{lac}\tau \tag{18}$$

where s_{lac} is the lactate concentration in the culture and $\tau = 2.2\ \mathrm{h^{-1}M^{-1}}$ obtained from linearizing the death rate dependence on lactate in a mammalian cell culture reported by S. Dhir et al.(Dhir et al., 2000). The maximum uptake rates of glucose and glutamine are $V_{glc} = 0.5$ mmol/gDW/h (Rodríguez-Enríquez et al., 2009) and $V_{gln} = 0.05$ mmol/gDW/h (Dhir et al., 2000).

Genome-scale metabolic network of CHO-K1

Finally we analyze the steady states of a genome scale model of the CHO-K1 line, based on the latest consensus reconstruction of CHO metabolism available at the time of writing (Hefzi et al., 2016). This metabolic network contains 4723 reactions (including exchanges) and 2773 metabolites (with cellular compartmentalization). It accounts for biomass synthesis through a virtual reaction that contains the moles of each metabolite required to synthesize one gram of biomass.

We employ the nutrients concentrations, c_i of Iscove's modified Dulbecco's medium (IMDM), a standard media formulation widely used in mammalian cell cultures. The enzymatic costs were obtained by T. Shlomi et al. from public repositories of enzymatic data. An estimate of the enzyme mass fraction $C = 0.078$ mg/mgDW was obtained for mammalian cells by the same authors (Shlomi et al., 2011). The maximum uptake rate of glucose was set at $V_{glc} = 0.5$ mmol/gDW/h, from previous models of CHO cells probed to experimental data (Kiparissides et al., 2011; Nolan & Lee, 2011).

We estimated that the uptake rates of amino acids are typically one order of magnitude slower than the uptake rate of glucose; ($V_i = V_{glc}/10$)(Dhir et al., 2000; Ozturk et al., 1992). We consider the cost of each amino acid per gram unit (w_i), according to the public Sigma Aldrich catalog. The maintenance energetic demand e_i is constant for each metabolite and was added in the form of an ATP hydrolysis drain at a flux rate 2.24868 mmol/gDW/h (Kilburn et al., 1969). In this model, we incorporate the effects of toxicity through the factor K

$$K = \frac{1}{(1 + s_{nh4}/K_{nh4})(1 + s_{lac}/K_{lac})} \tag{19}$$

where $K_{nh4} = 1.05$ mM, $K_{lac} = 8.00$ mM (Bree et al., 1988), s_{nh4} and s_{lac} are the concentrations of ammonia and lactate in the culture in the steady state reached. Finally, the effective cell growth rate is $\mu = Z \times K$.

Results

Simplified metabolic network

This is a metabolic network that by construction consumes only two nutrients: glucose and glutamine. We first optimize biomass production using as a reference medium the concentrations of these nutrients in the IMDM media. Then, for the rate of biomass production obtained we predict the optimum concentrations (in the sense of minimum cost of the substrate) that must be supplied to the culture at each steady state for different prices of glucose (w_g) and glutamine (w_q).

In Figure 3 we show the concentrations of glucose and glutamine for two different steady states of the culture. On the left, the culture is in a steady state with X =0.3 gDW/L and D =0.15 d^{-1}, and on the right, the culture is at the same rate of dilution but the cell density is higher, X =1.3

gDW/L. In both cases, the minimization of the cost guarantees that the resulting concentration of the metabolites are lower than the ones in the IMDM media represented by the green (glucose) and blue (glutamine) dashed lines. Moreover, depending on the relative costs between the nutrients it is possible to observe clear transitions in the concentrations to be supplied to the culture. Both at low and high cell density, when $w = \frac{w_g}{w_q} \geq 1.2$(i.e. when gln is more expensive than glc) the glutamine supplies must be stopped ($c_q = 0$) and the glucose concentration increased.

We also study the glucose and glutamine concentrations that must be supplied to the bioreactor for different values of the control parameter ξ (Fig.4). If the cost of glucose is larger than the cost of glutamine ($w_q < w_g$) (Fig.4a), the glutamine concentration is different from zero only for high cell density (high values of $\xi = X/D$). If glutamine is more expensive ($w_q > w_g$) (Fig.4b), the results suggest not to supply glutamine and to increase the glucose concentration. We can observe that for a wide range of ξ, the glucose concentration of IMDM (c_{g_0}) is much greater than necessary to guarantee growth. It is possible a notable reduction in the concentrations supplied having the cell in the same steady state.

The results presented in this section should not be understood in a quantitative manner. The metabolic network used, represents important biological processes in a cell, but it is nevertheless a crude abstraction of reality. Several metabolic pathways, fundamental to keep the cell functioning are not represented and this may justify the large space for optimization. However, they help to understand that the technique proposed is valid and provides meaningful results. In the next sections we test more realistic metabolic networks.

Genome-scale metabolic network of CHO-K1

In this section we study the optimal media formulation as a function of the steady state of the culture (parameterized by ξ), for the CHO-K1 cell-line. To be used as a reference for further discussions we show in Fig. 5, the effective growth rate μ and the cell density X as a function of ξ. It is important to recall here that, in accordance with pervious results (Fernandez-de-Cossío-Díaz et al., 2017), a given value of ξ defines an operational set-point for the cell culture, i.e., the cell metabolism in the culture. In other words, for a given cell type and medium, completely different fermentations (different volume and perfusion rates) will be metabolically equivalents for the same value of ξ. We also show in dashed lines the unstable zone of the phase diagram. The system is

stable in two regimes. In the first one there is high toxicity, low biomass yield and low cell density (Fernandez-de-Cossío-Díaz et al., 2017). In the second, the desirable one for the industry, cells are in an environment with no toxicity, high biomass yield and high cell density. In the later X decays as ξ increases.

In Fig.6 we show the optimum concentrations of the main metabolites supplied to the culture as a function of ξ and compare it with the concentrations in the IMDM culture. As the figure clearly shows, independently of the operation range of the chemostat (i.e., independently on ξ) most concentrations of the nutrients in the IMDM are overestimated, except glycine. Even more, according to these results, some nutrients are not even necessary for cell growth.

It can be appreciated that the optimal concentrations exhibit a non-trivial dependency with the control parameter ξ. For low values of ξ, (i.e., in the toxic region) where the dilution rate D is high, the cell density is very low and consequently the nutrient concentrations to guarantee a given X are also low. In the other stable regimen, the concentration of many metabolites first decreases with ξ, and then increases again with larger ξ. Other metabolites are unnecessary. This behaviour can be explained looking also to Fig.5. For $0.6 \geq \xi \leq 1$ the cell density X is maximum, and one needs to use a large variety of nutrients and in high concentrations to optimize the cost of the media. When X decreases, the concentrations may decrease again. However, for larger values of ξ, one needs to sustain a smaller number of cells and the optimization of the media is possible without using some expensive nutrients. Their absence is counter balanced by larger concentrations of other (cheaper) metabolites.

It is particularly important to check the consistency of our data with the literature. First, we remember that a microorganism is auxotrophic if it is capable of proliferating in a culture medium only if a specific substance has been added to it. Generally speaking CHO cells exhibit several amino acid auxotrophies (Naylor et al., 1979; Valle et al., 1973), the nine essential amino acids in humans (His, Ile, Leu, Lys, Met, Phe, Thr, Trp and Val) and arginine (Arg), which is also essential in rats for normal growth (Borman et al., 1946). In addition, CHO-specific auxotrophies include cysteine (Cys) and proline (Pro) (Duarte et al., 2014). As we observe in our results (Fig.6), all these amino acids must be supplied to the culture according to the simulation and its concentrations are different from zero. Furthermore, also glucose (Glc), tyrosine (Tyr) and glycine (Gly) must be added to the culture.

Looking in more detail to these plots it is worth to first discuss the absence of Glutamine in our optimized media. Glutamine, is an aminoacid consumed at high rate, therefore, it is usually overdosed in mammalian cell cultures and it is considered fundamental for optimal growth(Eagle, 1955). For example, many myeloma and hybridoma lines have an absolute requirement for glutamine. Glutamine, glutamate and asparagine play a big role in cell metabolism as protein constituents, nitrogen donors in nucleotide synthesis and important respiratory fuel (Duarte et al., 2014; Reitzer et al., 1979; Zielke et al., 1984). Glutamine depletion causes a severe decline in cell viability by apoptosis unless the cell line has glutamine synthetase activity and then glutamate is incorporate from culture medium to produce glutamine (Sanders & Wilson, 1984). Additionally, lack of glutamine trigger an increase in the glycolysis and affect the metabolism of other amino acids (Hagrot et al., 2017). However feeding excess glutamine induces high ammonium production in different cell cultures (Butler & Spier, 1984; Ljunggren & Häggström, 1992), reducing the viable cell density and the productivity (Hansen & Emborg, 1994; Hassell et al., 1991). Consequently, a number of established cell lines, like BHK-21, L-cells and CHO-K1, have been adapted to grow in glutamine-free media (Bort et al., 2010; Hassell et al., 1987; McDermott & Butler, 1993; Taschwer et al., 2012). Our simulations of the CHO-K1 line, remarkably, reproduce a perfectly functioning chemostat, for a medium free of glutamine for a wide range of values of ξ.

In our case the increase of glutamate and asparagine over IMDM levels was a palliative for the effect of glutamine lacking in medium optimized for $\xi \leq 1$ gDW d L^{-1}. Values of ξ above 1 gDW d L^{-1} could be difficult to attain due to the low growth rate of culture at this metabolic states. Very low growth rate trigger apoptosis signal leading to cell death (Sitton & Friedrich, 2008). There is experimental evidence suggesting that major glycine (Gly) addition could partially restore cell density and product formation observed in the absence of serine and glutamine (Duarte et al., 2014). In turn our optimization process suggests a notable increase of the Gly concentration in the media formulation (Fig.6). Gly, after of the glucose (Glc), is the cheaper amino acids according to the prices reported in the Sigma Aldrich catalogue. On the other hand; serine unavailability could affect culture growth as well, so, decreased level of serine were mirrored by increased amount of glycine. The same behavior was described by (Sellick et al., 2015).

Also, it has been proved that some intermediates of the TCA cycle (citrate, succinate, fumarate and malate) accumulate during culture phases, which indicates a bottleneck (Dickson, 2014). These

intermediates were observed to build up in the cell culture after the addition of a media, which contains pyruvate and amino acids (Asp, Asn, and Glu), and have been linked to growth limitation (Carinhas et al., 2013; Pereira et al., 2018; Sellick et al., 2011, 2015). Of course the quantitative character of these results should be interpret with caution, because on one side, the given stoichiometric matrix is only an approximation of the actual one, on the other, some amino acids may not be relevant for the metabolism of the cells, but still be used in other biological functions.

Finally, we evaluate the cost of the amino acids that are supplied to the culture, and compare the cost of the IMDM medium (estimated as $\sum w_i ci$) with the cost of the medium after the optimization. In Fig.7a we can observe a considerable decrease in the cost for all steady states that the system could reach. The cost of the optimal medium is at least one third of the cost of the IMDM medium (per liter unit).

On the other hand, in Fig.7b we show the relative cost of the production process (see Eq.(12)) as a function of ξ. When ξ increases the costs are similar and our results indicate that the efficient zone is achieved for steady states consistent with $0.6 \leq \xi \leq 1$. However, there is a wide range of operation where the overall production cost can be strongly reduced by optimizing the media. It is important to note that the first stable regimen ($\xi \ll 1$) is not optimum, despite the low value of cost production the cell density in this regime is very low.

Figure 8 shows the variation of the unitary production cost with the value of ξ (the operational set point) for a cell culture using the reference IMDM media. It can be observed that the production cost reaches an optimum minimal value around the value $\xi = 1$. However this value of ξ does not correspond to the maximum value of cell concentrations (see fig 8) and thus the maximum production yield. Therefore, our model predicts that to operate a optimal continuous fermentation of CHO cells, with a given fixed medium (IMDM here), an operational set-point (value of ξ between 0.6 and 1) must be selected. For ξ closer to 1 the unitary production cost is minimized, but for ξ values closer to 0.6 the product yield is maximized at the expenses of some extra cost. Engineer must select between one or other value of ξ, depending on other operational factors as: product demand, profitability margin, total capacity of production available and others.

Similarly, figure 9 shows the variation of the unitary production cost and the concentration of cells with the value of ξ (operational set point) in the CHO cell culture, but this time with the optimum medium predicted for each value of ξ. Medium optimization indeed reduces unitary

production cost. Note the values bellow 1 when production cost is normalized to the minimum production cost obtained with the reference IMDM medium. However, the qualitative dependence of the production cost and cell concentration remains similar to that depicted in figure 8. Optimal values of ξ are now between 0.6 and 0.9, a range just slightly narrow than before, but with the same potential conflict of interest for Engineers when selecting the operational set-point.

Other important aspect of our results, is that the optimal medium predicted is quite different for each operational set point in the culture, i.e value of ξ. Actually, the media optimization attained with the theoretical methods proposed here, is far from been just a mere reduction of possible excess in some medium components of the reference medium (see again figure 5). In the optimized medium, cell culture shows a different, optimal, metabolic state as compared to that in the reference medium for the same value of ξ. To illustrative this, figure 10 compares the metabolic fluxes in the culture with the reference IMDM and the optimized medium for $\xi = 0.7$.

Concluding remarks

Optimization of continuous fermentation process is based, generally, in decreasig the cell specific perfusion rate (CSPR) as much as possible. CSPR then is keeping in a minimum value which depends on the cell line nutritional requirement and nutritional depth of culture medium used (Konstantinov, 2006). In that case, the cell culture medium should be enriched in nutrient to allow the reduction of D without decreasing the cell concentration. In this way product concentration increases in the harvest, decreasing culture medium volume and production costs. Application of such optimization strategy, relay on the frequent use of cell bleeding of the bioreactor to artificially stabilize cell concentration. In other words the continuous culture is operated out of equilibrium. In our approach, instead, we attempt to optimize continuous culture operation, but in equilibrium. We compute the amino acid composition in the medium, which minimize production cost for a fixed cell concentration and likely product yield in equilibrium.

In this work we test this approach in-silico studying the metabolism of genome scale metabolic networks in continuous cell cultures and predict an optimum media formulation for this process. We analyzed the cellular metabolism in a chemostat by performing FBAwMC optimization coupled to the macroscopic variables of the bioreactor. We show that our results depend on the relationship between the cell density and the dilution rate ($\xi = X/D$) (Fernandez-de-Cossío-Díaz et al., 2017).

We optimize biomass production starting from a medium formulation widely used, IMDM, a highly enriched synthetic media well-suited for rapid proliferating and high-density cell cultures. Then, we cast the problem of media optimization within a Linear Programming framework in which the cost of the media should be minimized, constrained to maintain the same cell density in the chemostat as previously estimated for the reference medium. We also study the cost of the production process as a whole, to understand how the steady state of the culture determines the optimal mode of operation of the system. We exploit public data obtained from an economic evaluation performed in the Center of Molecular Immunlogy (CIM) at Habana, Cuba (Torriente, 2014) and show that this cost actually depends on the ratio: $\xi = X/D$.

We first studied a simplified metabolic model that exchanges glucose, glutamine and lactate with the culture and includes synthesis of precursors required for biomass formation, mitochondria OxPhos capacity, energy requirements of biomass biosynthesis, NADH production and maintenance energy, based on the parameters of the study performed by (Fernandez-de-Cossío-Díaz & Vazquez, 2017). We show that depending on the relative cost of glucose and glutamine, it is better to choose one medium or another. Remarkably, already in this simple model the results depend on the ration between the cell density X and the dilution rate D.

We also analysed genome scale models of mammalian cells. In particular the CHO-K1 line. We show that, in both cases, the medium can be optimized in for wide range of values of ξ. Also in both cases the cost of optimal medium formulation represents costs that are approximately one third of the cost of the IMDM medium, and still reproduce the same stable states. Finally, we also show that the optimal medium minimizes the cost of the whole production process at high cell densities.

We studied in detail the specificities of the CHO cell line. We show that the optimal media contains all the essential amino acids that are auxotrophic in CHO cells, such as His, Ile, Leu, Lys, Met, Phe, Thr, Trp, Val, Cys and Pro. We have found that most of the optimal nutrient concentrations are lower than in the IMDM media. On other hand, our results indicate that Asn, Gln, Asp and Glu only are necessary for high growth rate, and Ala and Ser are absolutely needless for cell growth. Glycine, on the other hand, seems a good substitute for more expensive nutrients.

At present, we don't pretend to give too much *quantitative* relevance to our results. Still, we are confident that the *qualitative* hallmarks of our simulations may be useful to guide the production of

new media. At first, they highlight the importance of the specificities of the metabolism of the cells when a media is selected. While this is certainly known by experimentalists our approach may help them saving time and resources when looking for optimal media. For example, our results suggest that, increasing the concentration of glycine and decreasing the presence of glutamine seems to be a reasonable strategy to decrease the cost of the standard media used in the industry for the CHO-K1 line.

More generally our results show that medium optimization for a continuous fermentation in equilibrium is highly dependent of the operational metabolic set-point in the cell culture (i.e. determined by the value $\xi = 1/CSPR$). Therefore, we predict that medium optimization in small non-continuous cell cultures could be misleading. Instead we support, following the results of (Fernandez-de-Cossío-Díaz et al., 2017), to model the metabolic behavior of large industrial bioreactor, in a small chemostat or a much smaller bioreactor operated in a continuos mode at the same operational set-point (value of ξ). The theoretical method proposed here, could be then used to guide a deep medium optimization at the small scale, and only then extrapolate to industrial scale. Note that for our method the selection of the initial reference medium shall be important, it determines the maximal cell concentrations attained (accessible) in the culture. Using a rich, although expensive, medium as initial reference medium shall be recommended.

These results rely on the validity of our assumptions. First of all we consider that the metabolic network studied should be a proper proxy for the behaviour of the cell lines. We have considered a homogeneous cell population in a well-mixed bioreactor, that provide reasonable fits to experimental data (Ben Yahia et al., 2015; Fernandez-de-Cossío-Díaz et al., 2017) but this may not be true in other realistic settings. Another important omission of this model is that we assume that the exchange of oxygen with the culture is not limited and does not limit cell growth. As a proof of concept we adopt a flux balance approach (Edwards et al., 2002), where cells are supposed to optimize their metabolism towards maximizing the growth rate. This may not be true in the industry, where cell lines may be optimized for productivity. However, this case can be easily introduced in our formalism. In addition, the quantitative predictions depend on the accuracy of the parameters found in the literature and databases.

References

Beg, Q. K., Vazquez, A., Ernst, J., de Menezes, M. A., Bar-Joseph, Z., Barabási, A.-L., & Oltvai, Z. N. (2007). Intracellular crowding defines the mode and sequence of substrate uptake by escherichia coli and constrains its metabolic activity. *Proceedings of the National Academy of Sciences*, *104*(31), 12663–12668. doi: 10.1073/pnas.0609845104

Ben Yahia, B., Malphettes, L., & Heinzle, E. (2015). Macroscopic modeling of mammalian cell growth and metabolism. *Applied Microbiology and Biotechnology*, *99*(17), 7009–7024. doi: 10.1007/s00253-015-6743-6

Borman, A., Wood, T. R., Black, H. C., Anderson, E. G., OESTEKLING, M., Womack, M., ... others (1946). The role of arginine in growth, with some observations on the effects of argininic acid. *Journal of Biological Chemistry*, *166*, 585–594.

Bort, J. A. H., Stern, B., & Borth, N. (2010). Cho-k1 host cells adapted to growth in glutamine-free medium by facs-assisted evolution. *Biotechnology journal*, *5*(10), 1090–1097. doi: 10.1002/biot.201000095

Bree, M. A., Dhurjati, P., Geoghegan, R. F., & Robnett, B. (1988). Kinetic modelling of hybridoma cell growth and immunoglobulin production in a large-scale suspension culture. *Biotechnology and Bioengineering*, *32*(8), 1067-1072. doi: 10.1002/bit.260320814

Brühlmann, D., Jordan, M., Hemberger, J., Sauer, M., Stettler, M., & Broly, H. (2015). Tailoring recombinant protein quality by rational media design. *Biotechnology progress*, *31*(3), 615–629. doi: 10.1002/btpr.2089

Butler, M., & Spier, R. (1984). The effects of glutamine utilisation and ammonia production on the growth of bhk cells in microcarrier cultures. *Journal of Biotechnology*, *1*(3-4), 187–196. doi: 10.1016/0168-1656(84)90004-X

Carinhas, N., Duarte, T. M., Barreiro, L. C., Carrondo, M. J., Alves, P. M., & Teixeira, A. P. (2013). Metabolic signatures of gs-cho cell clones associated with butyrate treatment and culture phase transition. *Biotechnology and bioengineering*, *110*(12), 3244–3257. doi: 10.1002/bit.24983

DeBerardinis, R. J., Mancuso, A., Daikhin, E., Nissim, I., Yudkoff, M., Wehrli, S., & Thompson, C. B. (2007). Beyond aerobic glycolysis: transformed cells can engage in glutamine metabolism that exceeds the requirement for protein and nucleotide synthesis. *Proceedings of the National Academy of Sciences*, *104*(49), 19345–19350. doi: 10.1073/pnas.0709747104

Dhir, S., Morrow, K. J., Rhinehart, R. R., & Wiesner, T. (2000, January). Dynamic optimization of hybridoma growth in a fed-batch bioreactor. *Biotechnology and Bioengineering*, *67*(2), 197-205. doi: 10.1002/(SICI)1097-0290(20000120)67:2<197::AID-BIT9>3.0.CO;2-W

Dickson, A. J. (2014). Enhancement of production of protein biopharmaceuticals by mammalian cell cultures: the metabolomics perspective. *Current opinion in biotechnology*, *30*, 73–79. doi: 10.1016/j.copbio.2014.06.004

Duarte, T. M., Carinhas, N., Barreiro, L. C., Carrondo, M. J. T., Alves, P. M., & Teixeira, A. P. (2014). Metabolic responses of CHO cells to limitation of key amino acids. *Biotechnology and Bioengineering*, *111*(10), 2095–2106. doi: 10.1002/bit.25266

Eagle, H. (1955). Nutrition needs of mammalian cells in tissue culture. *Science*, *122*(3168), 501–504. doi: 10.1126/science.122.3168.501

Edwards, J. S., Covert, M., & Palsson, B. (2002, March). Metabolic modelling of microbes: The flux-balance approach. *Environmental Microbiology*, *4*(3), 133-140. doi: 10.1046/j.1462-2920.2002.00282.x

Feist, A. M., & Palsson, B. O. (2010). The biomass objective function. *Current opinion in microbiology*, *13*(3), 344–349. doi: 10.1016/j.mib.2010.03.003

Fernandez-de-Cossío-Díaz, J., Leon, K., & Mulet, R. (2017, November). Characterizing steady states of genome-scale metabolic networks in continuous cell cultures. *PLOS Computational Biology*, *13*(11), e1005835. doi: 10.1371/journal.pcbi.1005835

Fernandez-de-Cossío-Díaz, J., & Vazquez, A. (2017, October). Limits of aerobic metabolism in cancer cells. *Scientific Reports*, *7*(1), 13488. doi: 10.1038/s41598-017-14071-y

Griffiths, J. (1992). Animal cell culture processes-batch or continuous? *Journal of biotechnology*, *22*(1-2), 21–30. doi: 10.1016/0168-1656(92)90129-W

Hagrot, E., Oddsdottir, H., Hosta, J., Jacobsen, E., & Chotteau, V. (2017). Poly-pathway model, a novel approach to simulate multiple metabolic states by reaction network-based model - application to amino acid depletion in cho cell culture. *Journal of Biotechnology*, *259*, 235-247. doi: 10.1016/j.jbiotec.2017.05.026

Hansen, H. A., & Emborg, C. (1994). Influence of ammonium on growth, metabolism, and productivity of a continuous suspension chinese hamster ovary cell culture. *Biotechnology progress*, *10*(1), 121–124. doi: 10.1021/bp00025a014

Hassell, T., Allen, I., Rowley, A., & Butler, M. (1987). The use of glutamine-free media for the growth of three cell lines in microcarrier culture. In *Modern approaches to animal cell technology* (pp. 245–263). Elsevier. doi: 10.1016/B978-0-408-02732-8.50023-7

Hassell, T., Gleave, S., & Butler, M. (1991). Growth inhibition in animal cell culture. *Applied biochemistry and biotechnology*, *30*(1), 29–41. doi: 10.1007/BF02922022

Hefzi, H., Ang, K. S., Hanscho, M., Bordbar, A., Ruckerbauer, D. E., Lakshmanan, M., ... Lewis, N. E. (2016, nov). A Consensus Genome-scale Reconstruction of Chinese Hamster Ovary Cell Metabolism. *Cell Systems*, *3*(5). doi: 10.1016/j.cels.2016.10.020

Henry, O., Kwok, E., & Piret, J. M. (2008). Simpler noninstrumented batch and semicontinuous cultures provide mammalian cell kinetic data comparable to continuous and perfusion cultures. *Biotechnology progress*, *24*(4), 921–931. doi: 10.1002/btpr.17

Ibarra, R. U., Edwards, J. S., & Palsson, B. O. (2002, November). Escherichia coli K-12 undergoes adaptive evolution to achieve in silico predicted optimal growth. *Nature*, *420*(6912), 186. doi: 10.1038/nature01149

Jerums, M., & Yang, X. (2005). Optimization of cell culture media. *BioProcess Int*, *3*(6), 38–44.

Kilburn, D., Lilly, M., & Webb, F. (1969). The energetics of mammalian cell growth. *Journal of cell science*, *4*(3), 645–654.

Kiparissides, A., Koutinas, M., Kontoravdi, C., Mantalaris, A., & Pistikopoulos, E. N. (2011). 'closing the loop' in biological systems modeling - from the in silico to the in vitro. *Automatica*, *47*(6), 1147–1155. doi: 10.1016/j.automatica.2011.01.013

Konstantinov, K., Goudar, C., Ng, M., Meneses, R., Thrifft, J., Chuppa, S., ... Naveh, D. (2006). The "push-to-low"approach for optimization of high-density perfusion cultures of animal cells. *Advances in biochemical engineering/biotechnology*, *101*, 75-98. doi: 10.1007/10_016

Konstantinov, K. B., & Cooney, C. L. (2015). White paper on continuous bioprocessing. may 20–21, 2014 continuous manufacturing symposium. *Journal of pharmaceutical sciences*, *104*(3), 813–820. doi: 10.1002/jps.24268

Ljunggren, J., & Häggström, L. (1992). Glutamine limited fed-batch culture reduces the overflow metabolism of amino acids in myeloma cells. *Cytotechnology*, *8*(1), 45–56.

McDermott, R., & Butler, M. (1993). Uptake of glutamate, not glutamine synthetase, regulates adaptation of mammalian cells to glutamine-free medium. *Journal of cell science*, *104*(1), 51–58.

Meleady, P., Doolan, P., Henry, M., Barron, N., Keenan, J., O'Sullivan, F., ... others (2011). Sustained productivity in recombinant chinese hamster ovary (cho) cell lines: proteome analysis of the molecular basis for a process-related phenotype. *BMC biotechnology*, *11*(1), 78. doi: 10.1186/1472-6750-11-78

Molenaar, D., Van Berlo, R., De Ridder, D., & Teusink, B. (2009). Shifts in growth strategies reflect tradeoffs in cellular economics. *Molecular systems biology*, *5*(1), 323. doi: 10.1038/msb.2009.82

Mullen, A. R., Wheaton, W. W., Jin, E. S., Chen, P.-H., Sullivan, L. B., Cheng, T., ... DeBerardinis, R. J. (2012). Reductive carboxylation supports growth in tumour cells with defective mitochondria. *Nature*, *481*(7381), 385. doi: 10.1038/nature10642

Naylor, S., Townsend, J., & Klebe, R. (1979). Characterization of naturally occurring auxotrophic mammalian cells. *Somatic cell genetics*, *5*(2), 271–277.

Nolan, R. P., & Lee, K. (2011, jan). Dynamic model of CHO cell metabolism. *Metabolic Engineering*, *13*(1), 108–124. doi: 10.1016/j.ymben.2010.09.003

Noor, E., Flamholz, A., Bar-Even, A., Davidi, D., Milo, R., & Liebermeister, W. (2016, November). The Protein Cost of Metabolic Fluxes: Prediction from Enzymatic Rate Laws and Cost Minimization. *PLOS Computational Biology*, *12*(11), e1005167. doi: 10.1371/journal.pcbi.1005167

Ozturk, S. S., Riley, M. R., & Palsson, B. Ø. (1992, feb). Effects of ammonia and lactate on hybridoma growth, metabolism, and antibody production. *Biotechnology and Bioengineering*, *39*(4), 418–431. doi: 10.1002/bit.260390408

Pereira, S., Kildegaard, H. F., & Andersen, M. R. (2018). Impact of cho metabolism on cell growth and protein production: an overview of toxic and inhibiting metabolites and nutrients. *Biotechnology journal*, *13*(3), 1700499. doi: 10.1002/biot.201700499

Reitzer, L. J., Wice, B. M., & Kenell, D. (1979). Evidence that glutamine, not sugar, is the major energy source for cultured hela cells. *The Journal of Biological Chemistry*, *254*(8), 2669-2676. doi: 10.1002/jcp.1041150316

Rodríguez-Enríquez, S., Marín-Hernández, A., Gallardo-Pérez, J. C., & Moreno-Sánchez, R. (2009). Kinetics of transport and phosphorylation of glucose in cancer cells. *Journal of cellular physiology*, *221*(3), 552–559. doi: 10.1002/jcp.21885

Sanders, P., & Wilson, R. (1984). Amplification and cloning of the chinese hamster glutamine synthetase gene. *The EMBO Journal*, *3*, 65-71. doi: 10.1002/j.1460-2075.1984.tb01762.x

Sellick, C. A., Croxford, A. S., Maqsood, A. R., Stephens, G., Westerhoff, H. V., Goodacre, R., & Dickson, A. J. (2011). Metabolite profiling of recombinant cho cells: designing tailored feeding regimes that enhance recombinant antibody production. *Biotechnology and bioengineering*, *108*(12), 3025–3031. doi: 10.1002/bit.23269

Sellick, C. A., Croxford, A. S., Maqsood, A. R., Stephens, G. M., Westerhoff, H. V., Goodacre, R., & Dickson, A. J. (2015). Metabolite profiling of cho cells: Molecular reflections of bioprocessing effectiveness. *Biotechnology journal*, *10*(9), 1434–1445. doi: 10.1002/biot.201400664

Sheikh, K., Förster, J., & Nielsen, L. K. (2005, September). Modeling Hybridoma Cell Metabolism Using a Generic Genome-Scale Metabolic Model of Mus musculus. *Biotechnology Progress*, *21*(1), 112-121. doi: 10.1021/bp0498138

Shlomi, T., Benyamini, T., Gottlieb, E., Sharan, R., & Ruppin, E. (2011, March). Genome-Scale Metabolic Modeling Elucidates the Role of Proliferative Adaptation in Causing the Warburg Effect. *PLOS Computational Biology*, 7(3), e1002018. doi: 10.1371/journal.pcbi.1002018

Sitton, G., & Friedrich, S. (2008). Mammalian cell culture scale-up and fed-batch control using automated flow cytometry. *Journal of Biotechnology*, *135*, 174-180. doi: 10.1016/j.jbiotec.2008 .03.019

Taschwer, M., Hackl, M., Bort, J. A. H., Leitner, C., Kumar, N., Puc, U., ... others (2012). Growth, productivity and protein glycosylation in a cho epofc producer cell line adapted to glutamine-free growth. *Journal of biotechnology*, *157*(2), 295–303. doi: 10.1016/j.jbiotec.2011.11.014

Torriente, Y. G. (2014). *Evaluación técnico-económica de la producción del Nimotuzumab a escala de 2000 L* (Unpublished master's thesis). Facultad de Ingeniería Química, CUJAE. Centro de Inmunología Molecular.

Valle, D., Downing, S. J., Harris, S. C., & Phang, J. M. (1973). Proline biosynthesis: multiple defects in chinese hamster ovary cells. *Biochemical and biophysical research communications*, *53*(4), 1130–1136. doi: 10.1016/0006-291X(73)90582-2

van Hoek, M. J., & Merks, R. M. (2012). Redox balance is key to explaining full vs. partial switching to low-yield metabolism. *BMC systems biology*, *6*(1), 22. doi: 10.1186/1752-0509-6-22

Varma, A., & Palsson, B. (1994). Metabolic flux balancing: basic concepts, scientific and practical use. *Bio/Technology*, *12*, 994–998. doi: 10.1038/nbt1094-994

Vazquez, A., & Oltvai, Z. N. (2011, April). Molecular Crowding Defines a Common Origin for the Warburg Effect in Proliferating Cells and the Lactate Threshold in Muscle Physiology. *PLOS ONE*, *6*(4), e19538. doi: 10.1371/journal.pone.0019538

Vazquez, A., & Oltvai, Z. N. (2016). Macromolecular crowding explains overflow metabolism in cells. *Scientific reports*, *6*, 31007. doi: 10.1038/srep31007

Werner, R. G., Walz, F., Noé, W., & Konrad, A. (1992). Safety and economic aspects of continuous mammalian cell culture. *Journal of biotechnology*, *22*(1-2), 51–68. doi: 10.1016/0168-1656(92) 90132-S

Zielke, H., Zielke, C., & Ozand, P. (1984). Glutamine: a major energy source for cultured mammalian cells. *Federation Proceedings*, *43*(1), 121-125. doi: 10.1002/jcp.1041150316

Figure legends

Figure 1: Cell culture in continuous mode

A cell culture is grown in a tank that is continuously fed with a constant flux (blue arrows) of fresh media coming from a reservoir. An equivalent flux carries used media and cells away from the culture tank, maintaining a constant volume in the culture. The effluent contains cells, secreted metabolites and unused substrates. The figure displays the simple case of no cell retention (chemostat). Notation: substrate concentrations in media reservoir (c_i), cell density and metabolite concentrations in the culture (X, s_i), dilution rate ($D = F/V$, where F is the input/output flux and V the culture volume).

Figure 2: Simplified model of the metabolism of a mammalian cell

Lower-case letters without a prime denote precursor requirements to duplicate a cell, using the one-letter nomenclature for amino acids, x for AcCoA and z for glucose. Upper-case letters denote the uptake of glucose (G), secretion of lactate (L), uptake of glutamine (Q), dehydrogenase flux (red arrows with reverse dashed, N), ATP synthesis (A) and total transaminase (blue arrows, T). The primed variables are the isocitrate dehydrogenase flux (E') and the production rate of glutamine derived from glutamate (glutamine synthase, Q'). The dashed reactions are reversed under a limitation of OxPhos capacity. Generation and consumption of ATP is indicated by filled and empty black circles, respectively.

Figure 3: Nutrient concentrations vs. w for the simplified metabolic network

Optimum concentrations of glucose c_g (continuous green line) and glutamine c_q (continuous blue line) in function of costs $w = w_g/w_q$ for two different steady states. Left, lower cell density and right, higher cell density. In right, horizontal dashed lines represent fixed concentrations of IMDM media, c_{g_0} (green) and c_{q_0} (blue). Vertical lines show the values of w where a transition occurs in nutrients concentrations.

Figure 4: Nutrient concentrations vs. ξ for the simplified metabolic network

Optimum concentrations of glucose c_g (continuous green line) and c_q (continuous blue line) as function of ξ for a fixed dilution rate, D =0.20 d^{-1}. Horizontal dashed lines represent the constant

concentrations of IMDM media, c_{g_0} (green) y c_{q_0} (blue). Left, glucose is more expensive than glutamine (w =0.5); and right, glucose is cheaper than glutamine (w =2.0).

Figure 5: Cell density and effective cell growth rate for the simplified metabolic network

Cell density and effective cell growth rate as a function of ξ, using the IMDM media.

Figure 6: Culture media for the Genome-scale metabolic network of CHO-K1

Main metabolites concentrations supplied to the culture as a function of ξ. Red lines represent IMDM medium and green lines correspond to optimum media.

Figure 7: Media cost and Unitary cost of the production process

7a Media cost as a function of ξ, using fixed media (red line, IMDM media) and with optimum media (green line). 7b Unitary cost of the production process using the optimum media divided by the cost using IMDM media as a function of ξ.

Figure 8: Cost of the production process using IMDM media

Cost of the production process using IMDM media divided by the minimum value of the cost reached using the same media (red) and the cell density (gray) as a function of ξ.

Figure 9: Comparison of production process costs using IMDM and optimized media

Cost of the production process using the optimum media divided by the minimum value of the cost reached using the IMDM media (green) and the cell density (gray) as a function of ξ.

Figure 10: Comparison of specific uptake rate using IMDM and optimized media

Specific uptake rate by some metabolites for the value of $\xi = .7$, where the cost of production is minimum, using optimum media (green) and IMDM media (red).

Figures

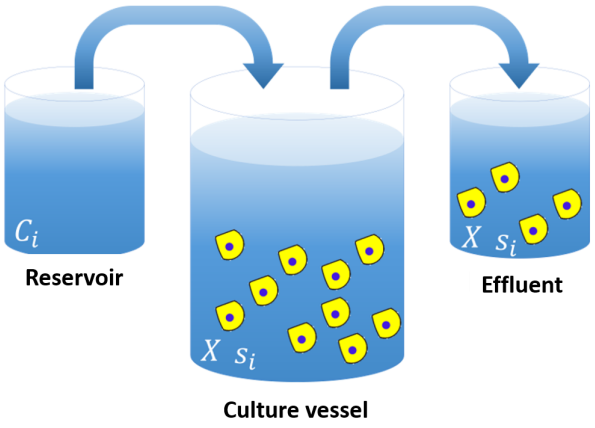

Figure 1

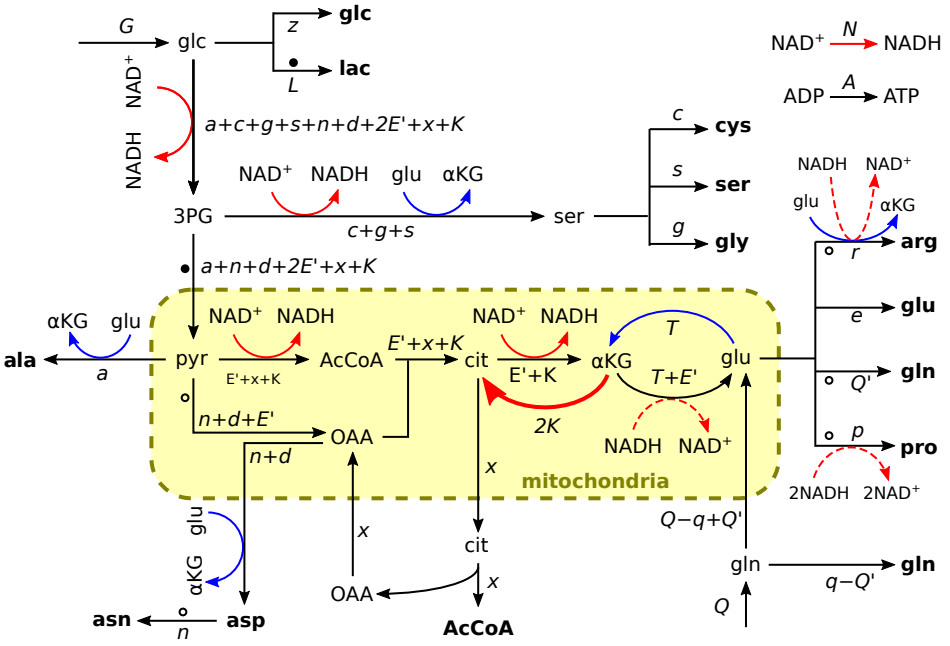

Figure 2

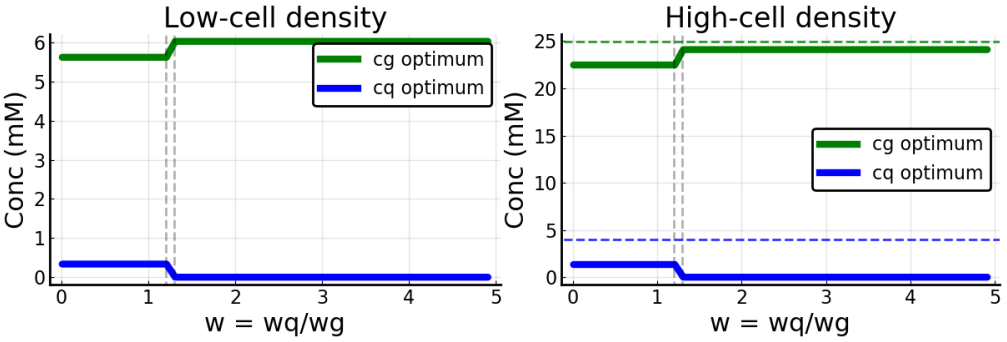

Figure 3

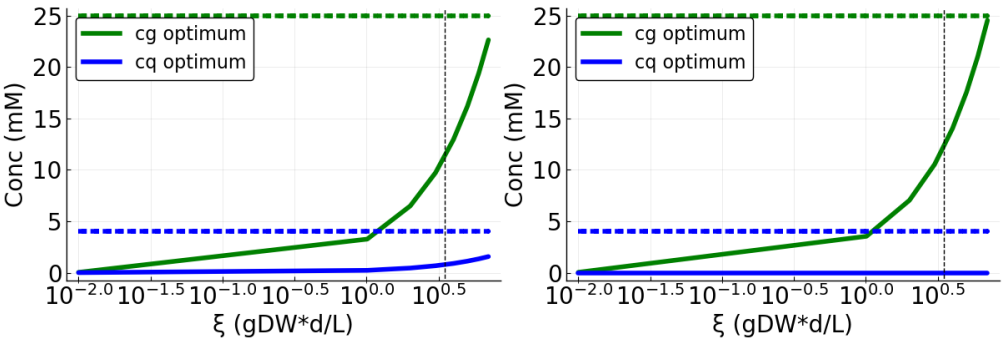

(a) $w = 0.5$ (b) $w = 2.0$

Figure 4

(a) Effective cell growth rate (b) Cell density

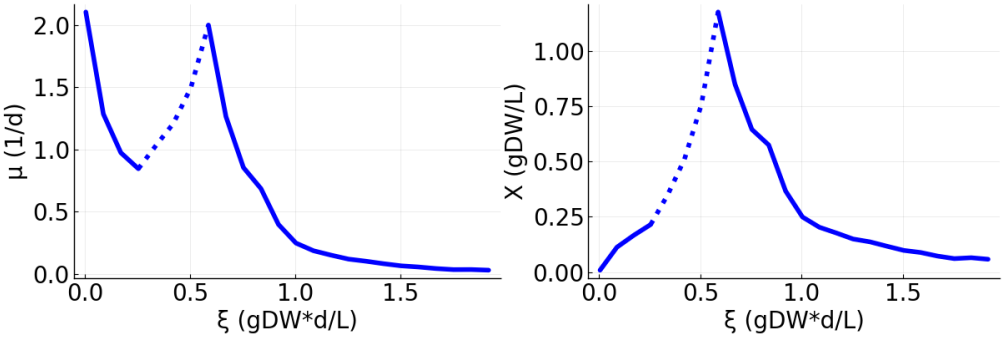

Figure 5

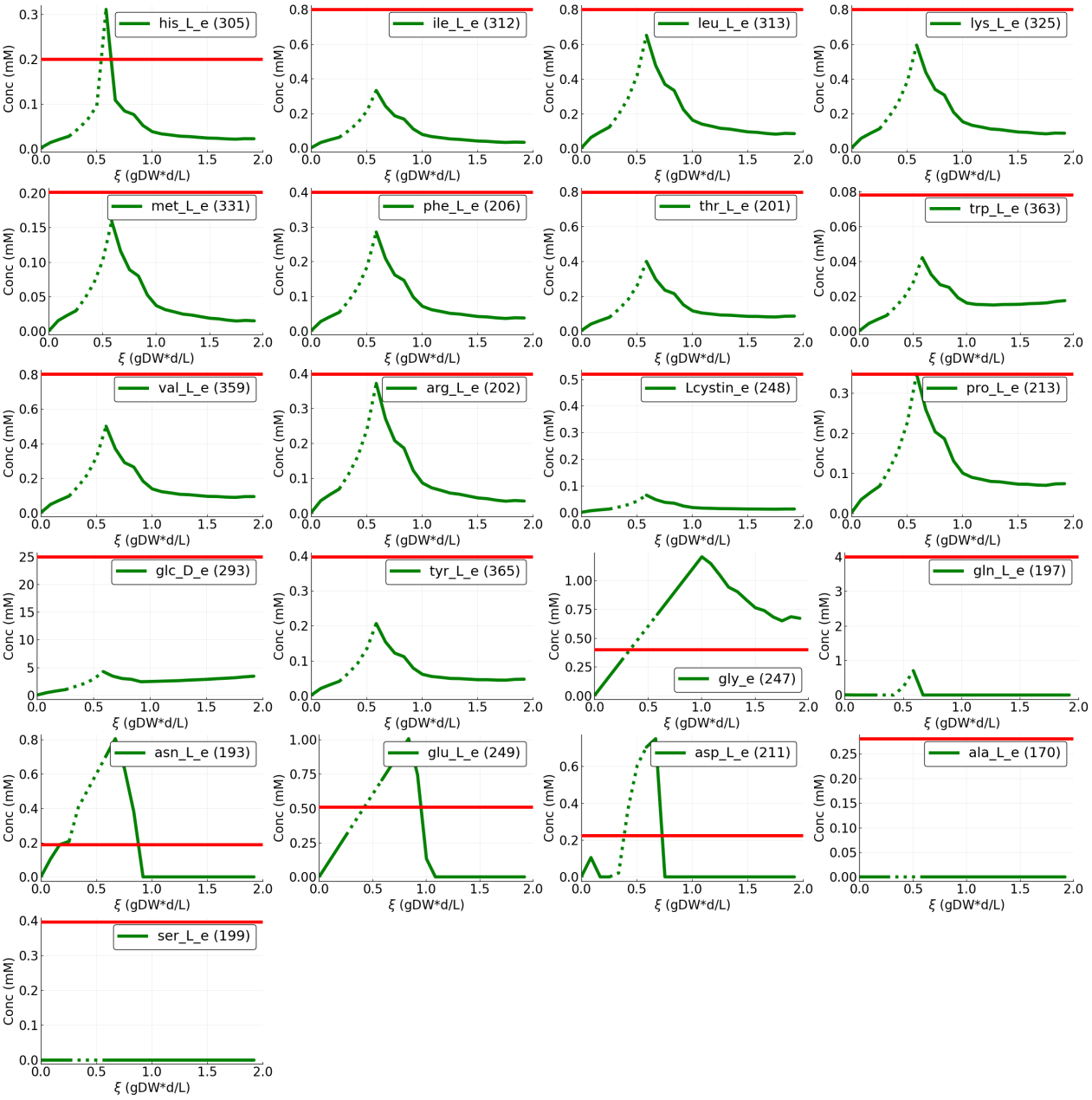
his_L_e (305)
ile_L_e (312)
leu_L_e (313)
lys_L_e (325)
met_L_e (331)
phe_L_e (206)
thr_L_e (201)
trp_L_e (363)
val_L_e (359)
arg_L_e (202)
Lcystin_e (248)
pro_L_e (213)
glc_D_e (293)
tyr_L_e (365)
gly_e (247)
gln_L_e (197)
asn_L_e (193)
glu_L_e (249)
asp_L_e (211)
ala_L_e (170)
ser_L_e (199)
Conc (mM)
ξ (gDW*d/L)

Figure 6

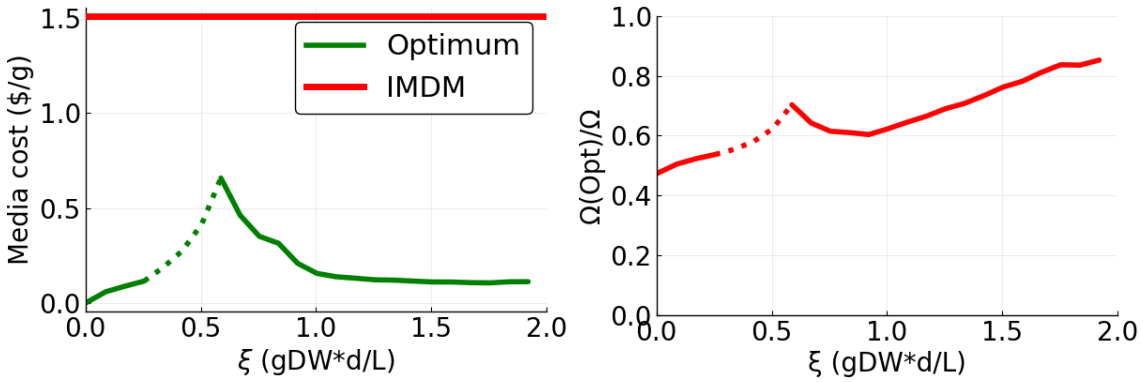

(a) (b)

Figure 7

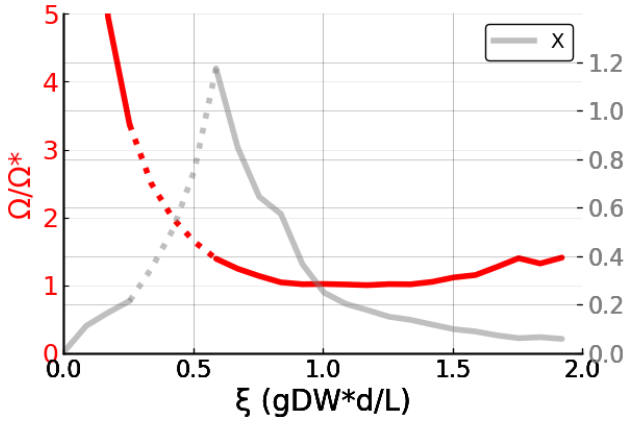

Figure 8

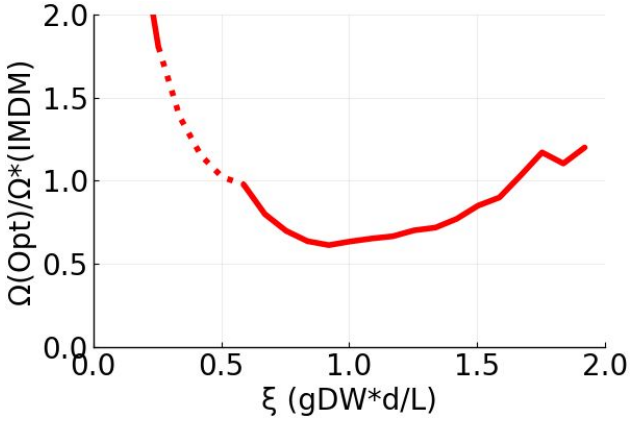

Figure 9

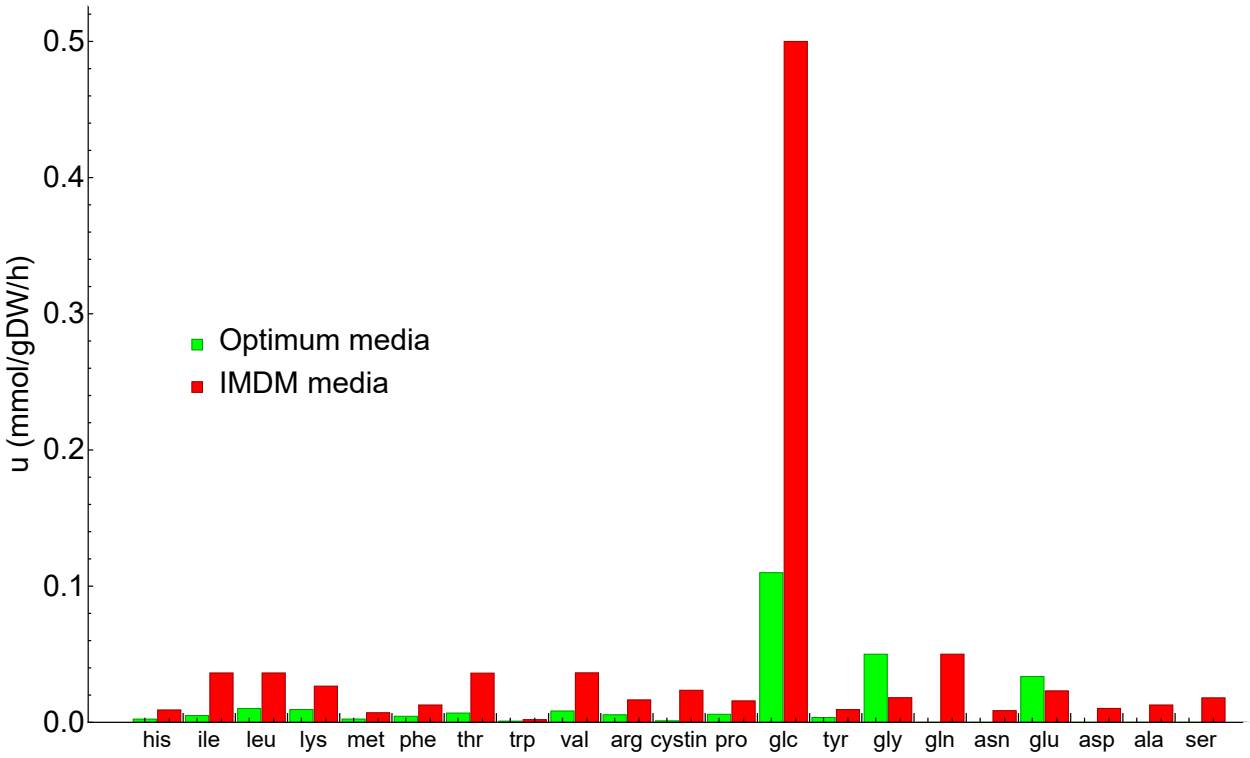
0.5
0.4
0.3
0.2
0.1
0.0
u (mmol/gDW/h)
Optimum media
IMDM media
his
ile
leu
lys
met
phe
thr
trp
val
arg
cystin
pro
glc
tyr
gly
gln
asn
glu
asp
ala
ser

Figure 10